INFECTION AND IMMUNITY, Sept. 2005, p. 5379–5387 Vol. 73, No. 9
0019-9567/05/$08.00+0 doi:10.1128/IAI.73.9.5379–5387.2005

Gliding Motility Leads to Active Cellular Invasion by *Cryptosporidium parvum* Sporozoites

Dawn M. Wetzel,[1]† Joann Schmidt,[2] Mark S. Kuhlenschmidt,[2] J. P. Dubey,[3] and L. David Sibley[1]*

Department of Molecular Microbiology, Washington University School of Medicine, 660 S. Euclid Ave., St. Louis, Missouri 63110[1]; Department of Pathobiology, College of Veterinary Medicine, University of Illinois at Urbana-Champaign, 2001 S. Lincoln Ave., Urbana, Illinois 61801[2]; and Animal Parasitic Diseases Lab, BARC-East, Bldg. 1001, ANRI, Agricultural Research Service, USDA, Beltsville, Maryland 20705[3]

Received 7 February 2005/Returned for modification 25 March 2005/Accepted 19 April 2005

We examined gliding motility and cell invasion by an early-branching apicomplexan, *Cryptosporidium parvum*, which causes diarrheal disease in humans and animals. Real-time video microscopy demonstrated that *C. parvum* sporozoites undergo circular and helical gliding, two of the three stereotypical movements exhibited by *Toxoplasma gondii* tachyzoites. *C. parvum* sporozoites moved more rapidly than *T. gondii* sporozoites, which showed the same rates of motility as tachyzoites. Motility by *C. parvum* sporozoites was prevented by latrunculin B and cytochalasin D, drugs that depolymerize the parasite actin cytoskeleton, and by the myosin inhibitor 2,3-butanedione monoxime. Imaging of the initial events in cell entry by *Cryptosporidium* revealed that invasion occurs rapidly; however, the parasite does not enter deep into the cytosol but rather remains at the cell surface in a membrane-bound compartment. Invasion did not stimulate rearrangement of the host cell cytoskeleton and was inhibited by cytochalasin D, even in host cells that were resistant to the drug. Our studies demonstrate that *C. parvum* relies on a conserved actin-myosin motor for motility and active penetration of its host cell, thus establishing that this is a widely conserved feature of the Apicomplexa.

The Apicomplexa is a large phylum of obligately intracellular parasites of medical and veterinary importance. The life cycles of all apicomplexans contain one or more haploid invasive stages and a diploid stage that is the result of a sexual cycle (11). *Toxoplasma gondii*, the causative agent of toxoplasmosis in neonates and the immunocompromised, has two tissue stages, tachyzoites and bradyzoites, within its life cycle (29). In all members of the phylum, the stage that emerges from oocysts after sexual recombination is termed a sporozoite. Sporozoites are also invasive and give rise to infection of intestinal enterocytes following oral ingestion by susceptible hosts. In *Cryptosporidium* spp., the sporozoite (contained within a thick-walled oocyst) is primarily responsible for transmission between hosts. Amplification of parasites within the host is the result of two cycles involving successive replication and invasion by merozoites and sporozoites (derived from thin-walled oocysts).

The members of the phylum Apicomplexa that commonly cause disease in humans include *T. gondii*; *Plasmodium* spp., the causative agents of malaria; and *Cryptosporidium* spp., agents of waterborne diarrhea that are particularly dangerous for those with immune deficiencies. Although the medical importance of *Cryptosporidium* spp. is well understood, the cellular and molecular mechanisms of infection by these organisms are poorly characterized, mostly due to their intractability (7). *Cryptosporidium* spp. are difficult to propagate in tissue culture, and no system for genetic study exists (23). Most of our understanding of the cellular biology of *Cryptosporidium* spp. is inferred from other members of the Apicomplexa, particularly *T. gondii*, which has been a model for this group (30). However, *Cryptosporidium* is an early-branching apicomplexan, more similar to gregarines (parasites of invertebrates) than to either *Toxoplasma* or *Plasmodium* (6), and thus may differ in fundamental features such as motility and invasion.

Cryptosporidium does not penetrate deeply into the cytosol of its host cell but rather rests on a pedestal of actin filaments that forms at the apical surfaces of epithelial cells of the gut (7). Enclosed with the host cell plasma membrane, *Cryptosporidium* remains intracellular but extracytoplasmic. Previous studies on the interaction of *Cryptosporidium* sporozoites with host cells reveal a substantial rearrangement of the host cell cytoskeleton following infection (14, 15). This response stands in marked contrast to invasion by *T. gondii*, which is independent of host cell actin (9, 28). Entry by *T. gondii* and *Plasmodium* spp. is extremely fast, occurring in less than 1 min (28, 35). However, previous studies of *Cryptosporidium* infection examined the interaction only at 24 h or later after addition of parasites to host cells. As such, the events that lead to initial entry of *Cryptosporidium* into epithelial cells remain uncharacterized.

Apicomplexans are thought to advance upon a target host cell for invasion using a unique, active process termed gliding motility. Gliding motility by apicomplexans does not require shape changes like the crawling of amoebae, nor do these parasites have cilia or flagella, except in the microgamete life cycle stage (24). Instead, the motility of most stages appears to be driven by coupling the translocation of surface adhesins to an actin-myosin motor beneath the parasite plasma membrane

* Corresponding author. Mailing address: Department of Molecular Microbiology, Campus Box 8230, Washington University School of Medicine, St. Louis, MO 63110. Phone: (314) 362-8873. Fax: (314) 362-3203. E-mail: sibley@borcim.wustl.edu.

† Present address: Pediatrics Residency Program, Children's Hospital of New York, 630 W. 168th St., New York, NY 10032.

(32). For *T. gondii* tachyzoites, genetic studies show that only parasite actin is required for cell invasion (9). Unlike mammalian cells, which retain 50% of their actin pool as filaments, *T. gondii* maintains the vast majority of its actin (97%) in the monomeric state (8). Induction of polymerization of actin with the drug jasplakinolide (JAS) causes *T. gondii* tachyzoites to form a projection of apical actin filaments (31). Treatment with JAS also increases the rate of *T. gondii* tachyzoite gliding; however, these movements are aberrant due to frequent direction reversals (36). Collectively, these findings indicate that polymerization of new actin filaments controls both the initiation and the directionality of motility.

In *T. gondii* tachyzoites, motility consists of three stereotypical behaviors: (i) circular gliding, which occurs only in a counterclockwise direction; (ii) upright twirling, which occurs only in a counterclockwise direction; and (iii) helical gliding, which uses a clockwise revolution to move the crescent-shaped parasite forward across its substrate (19). Gliding motility in other apicomplexans has been demonstrated by trail assays with *C. parvum* (2) and *Eimeria* spp. (16) as well as by video microscopy studies of gliding *Plasmodium berghei* (18) or beads moving along the surfaces of gregarines (25). While the mechanism and the stereotypical movements of gliding motility are believed to be conserved throughout the Apicomplexa (32), there are no published studies of the process in real time in *Cryptosporidium* spp. or in *T. gondii* sporozoites.

In the studies reported here, we characterize gliding motility by *C. parvum* sporozoites and *T. gondii* sporozoites and compare it to the well-studied motility of tachyzoites. We also demonstrate that invasion by *Cryptosporidium* relies on the same actin-dependent motility mechanism that allows the parasite to become enveloped within the host cell membrane.

MATERIALS AND METHODS

***T. gondii* tachyzoite culture.** *T. gondii* strain RH tachyzoites were propagated in human foreskin fibroblast monolayers as described previously (28). Parasites were obtained soon after host cell lysis. All cultures were tested with the GenProbe (San Diego, CA) mycoplasma detection system and found to be free of mycoplasma.

Purification of *C. parvum* sporozoites. *C. parvum* sporozoites were excysted from oocysts purified from the feces of infected calves as described elsewhere (33). Briefly, oocysts were removed from media containing antimicrobial and antifungal agents by centrifugation at 16,000 × *g* at room temperature in an Eppendorf model 1415C centrifuge (Brinkmann Instruments, Inc., Westbury, NY) and rinsed with Hanks balanced salt solution (HBSS) (Life Technologies, Gaithersburg, MD). Oocysts were incubated in 1% sodium hypochlorite for 10 min at 4°C and rinsed four to five times with HBSS by centrifugation until the pH indicator returned to a pink color. Next, oocysts were incubated at 37°C for 1 h. Sodium taurocholate (Sigma, St. Louis, MO) was added to 1.5%, trypsin (Life Technologies) was added to 0.5%, and parasites were returned to 37°C for 15 min to 1 h. Every 15 min, oocysts were screened by light microscopy to determine the ratio of sporozoites to intact oocysts. Once sporozoites were approximately 10 times more prevalent than intact oocysts, they were resuspended in Ringer's solution (155 mM NaCl, 3 mM KCl, 2 mM $CaCl_2$, 1 mM $MgCl_2$, 3 mM NaH_2PO_4, 10 mM HEPES, 10 mM glucose) and used for video microscopy experiments.

Purification of *T. gondii* sporozoites. The excystation procedure for *T. gondii* sporozoites was modified from previously reported protocols (26). Briefly, *T. gondii* oocysts (strain ME49, clone B7) in a 2% sulfuric acid solution were semipurified from the feces of infected cats (12). They were pelleted at 450 × *g* for 10 min in an Eppendorf model 5810R centrifuge (Brinkmann Instruments, Inc.) and washed three times with HBSS containing 0.001 M EGTA and 0.01 M HEPES at pH 7.2 (HHE). The oocysts were sterilized in 10 ml of 0.5% sodium hypochlorite in phosphate-buffered saline (PBS) for 30 min at 0°C, pelleted at 450 × *g* for 10 min, rinsed four times with HHE, and stored for ≤2 weeks at 4°C until needed for experiments.

Glass beads (450 to 600 μm; Sigma) were added to oocysts, and tubes were vortexed three times at maximum speed for 45 to 60 s. The beads were allowed to settle, the supernatant was removed, and the pellet was washed twice with HHE. The combined supernatant and washes were pelleted at 450 × *g*, resuspended in excysting medium (5% sodium taurocholate in HHE at pH 7.5), and incubated at 37°C for 30 min. After excystation, fetal bovine serum (FBS) was added to the parasites to a 10% final concentration, and the preparations were centrifuged for 10 min at 450 × *g*. Sporozoites were rinsed twice in HHE and then resuspended in media for the experiments described below.

Trail formation assay. Coverslips were coated in 10 μg/ml poly-L-lysine (PLL) in PBS for 30 min at room temperature and rinsed in PBS. Freshly excysted *C. parvum* sporozoites were resuspended in Ringer's solution, added to precoated coverslips, and incubated at 37°C for 30 min. Slides were fixed in −20°C methanol (Fisher Scientific) and blocked with 20% FBS in PBS. The presence of the surface membrane protein p25 in trails was detected with mouse monoclonal antibody (MAb) 3E3 (1:50) (Biodesign International, Saco, ME). Primary antibody labeling was detected using a secondary goat anti-mouse antibody directly conjugated to Oregon Green (1:250; Molecular Probes, Eugene, OR). Coverslips were rinsed, mounted in Vectashield containing 4′,6′-diamidino-2-phenylindole (DAPI) (Vector Laboratories, Burlingame, CA), and examined with wide-field fluorescence microscopy using an upright Zeiss Axioscope (Carl Zeiss Microimaging, Inc., Thornwood, NY).

Invasion assay. KB100 or CYT1 (cytochalasin D [CD]-resistant) epithelial cells (34), or MDCK cells (ATCC CCL34) were plated on glass coverslips 24 h before experiments. *C. parvum* oocysts were excysted, resuspended in Ringer's solution with 2 μM dimethyl sulfoxide (DMSO) or 2 μM CD (EMD Biosciences, La Jolla, CA), and added to coverslips containing host cell monolayers. Coverslips were incubated for 5 min at 37°C to allow for invasion, fixed in 4% formaldehyde in PBS at room temperature for 15 min, labeled with MAb 3E3, and detected with a secondary goat anti-mouse antibody conjugated to Alexa 594 (Molecular Probes, Eugene, OR). Cells were then permeabilized with 0.1% saponin in 20% FBS in PBS, and parasites were labeled with MAB 3E3 and detected with a secondary goat anti-mouse antibody conjugated to Alexa 488 (Molecular Probes). Host cell actin was labeled with phalloidin directly conjugated to Alexa 350 (Molecular Probes). Coverslips were rinsed, mounted in Vectashield, and examined by wide-field fluorescence microscopy. For quantification, 100 parasites per coverslip were examined by fluorescence and the number of red (external) versus green (internal) parasites was recorded for each of two coverslips per experiment. Data shown are means ± standard errors (SE) for three experiments.

Immunofluorescence detection of apical projections. *T. gondii* sporozoites were isolated, resuspended in Ringer's solution, and treated with 2 μM JAS (Molecular Probes) for 10 min. Parasites were allowed to settle on coverslips precoated for 30 min with PLL. Coverslips were fixed in 100% methanol, blocked with 50% FBS in PBS, and labeled with mouse monoclonal antibody C4 (Cytoskeleton, Denver, CO) against actin. Primary antibody labeling was detected using a secondary goat anti-mouse antibody directly conjugated to Texas Red (1:250; Molecular Probes). Coverslips were rinsed, mounted in Vectashield plus DAPI, and examined by wide-field fluorescence microscopy.

Video microscopy. Freshly isolated parasites were resuspended in Ringer's solution containing 1% FBS, treated with either 2 μM JAS, 1 μM latrunculin B (LatB) (Molecular Probes), 1 μM CD, 10 μM 2,3-butanedione monoxime (BDM) (EMD Biosciences, San Diego, CA), or 1% DMSO (Sigma), and allowed to glide on glass-bottom dishes (MatTek Corp., Ashland, MA) precoated with either 100% FBS for *T. gondii* or PLL for *C. parvum* (our unpublished observations indicate that this parasite does not adhere to FBS-coated glass) at room temperature for 30 min. Video microscopy was conducted using a Zeiss Axiovert equipped with phase-contrast and epifluorescence microscopy and a temperature-controlled stage (Medical Systems Corp., Greenvale, N.Y.) to maintain 37°C incubation as described previously (28). The optical path in this microscope is corrected to simulate an upright orientation so that objects appear in their true orientation with respect to the *x* and *y* planes. Motility was recorded beginning with the addition of drug-treated parasites to the heated chamber and continuing for up to 45 min.

Time lapse images and the supplemental videos were collected under low-light illumination with a Hamamatsu ORCA ER camera (Hamamatsu Photonics KK, Hamamatsu, Japan). Videos were recorded digitally at approximately 8 frames per s with Openlabs v4.0.1 (Improvision, Lexington, MA), cropped, and saved as Quicktime v6.5.1 movies (Apple). Frames used to create the time lapse series were taken from Quicktime movies and processed using Adobe Photoshop v6 (Adobe, San Jose, CA).

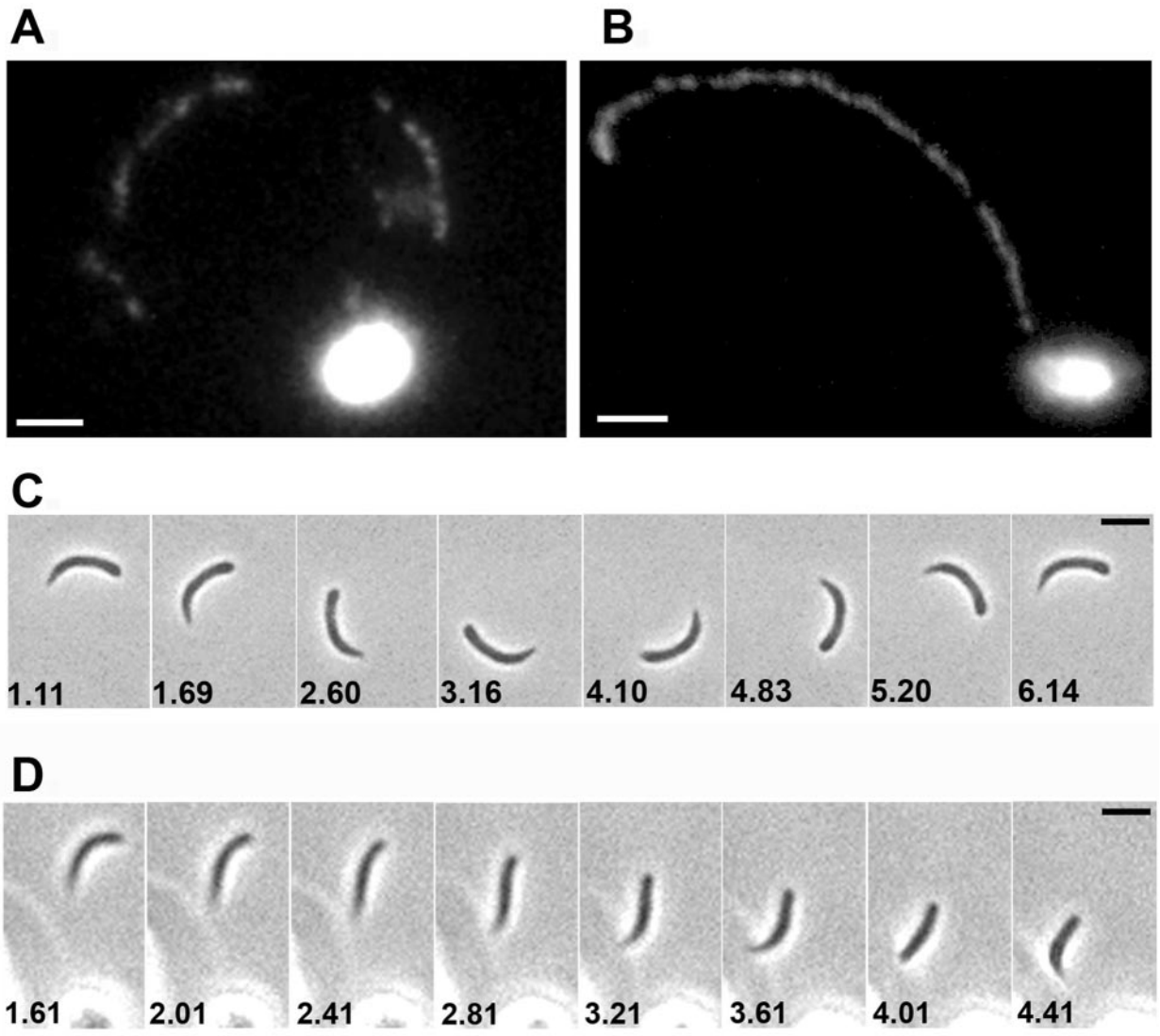

FIG. 1. Gliding motility by *C. parvum* sporozoites. (A and B) *C. parvum* deposited surface membrane trails during gliding on a solid substrate. (Panels A and B show two separate examples.) Trails were visualized by immunofluorescence microscopy using an antibody to the surface protein p25 (mouse monoclonal antibody 3E3) and a secondary anti-mouse antibody conjugated to Oregon Green. Bar, 5 μm. (C and D) Time lapse phase-contrast video microscopy allowed visualization of gliding motility by *C. parvum* in real time. Shown are series of frames from movies of circular gliding (video 1) (C) and helical gliding (video 2) (D) by *C. parvum* sporozoites. Time elapsed is shown in seconds in the lower left corner of each frame. Bars, 5 μm.

For all rate analyses, three separate experiments, each containing five examples of the type of motility under study from two or more separate dishes, were analyzed. The number of 360-degree revolutions per second was used to determine the twirling rate. The total distance traveled in a 10-s period of uninterrupted locomotion was used to determine rates for circular and helical gliding. Averages shown in tables are means ± SE and were analyzed for statistical significance by Student's two-tailed *t* test.

RESULTS

***C. parvum* sporozoites form trails during gliding.** Previous immunofluorescence studies indicate that *C. parvum* forms circular trails while gliding (2). To examine the pattern of trails formed by *C. parvum* on the substrates used here, we performed a gliding assay. *C. parvum* sporozoites were allowed to glide on PLL-coated coverslips and then were processed for immunofluorescence. Trail deposition was visualized using an antibody to the surface membrane protein p25. *C. parvum* sporozoites deposited trails that formed both circular and helical patterns (Fig. 1A and B), as previously reported for *T. gondii* tachyzoites.

Real-time analysis of *C. parvum* motility. Because the trail assays described above could not show the rate or pattern of gliding, we conducted real-time video microscopy studies to further examine motility by *C. parvum* sporozoites. We found that *C. parvum* exhibited similar motility to *T. gondii*. Although we could not identify episodes of upright twirling, *C. parvum* did exhibit counterclockwise circular movements (Fig. 1C; see also video 1) (all videos are available at http://www.sibleylab.wustl.edu/cptgmovies/) and directional helical gliding (Fig. 1D

TABLE 1. Gliding by *C. parvum* sporozoites

Behavior	Motility of:			
	T. gondii tachyzoites		*C. parvum* sporozoites	
	Occurrence[a]	Rate[b,c] (mean ± SE)	Occurrence[a]	Rate[b,d] (mean ± SE)
Twirling (clockwise)	+	0.37 ± 0.08	−	NA[e]
Circular gliding	+	0.98 ± 0.19	+	4.92 ± 0.15*
Helical gliding	+	1.64 ± 0.12	+	5.31 ± 1.17*
Rolling	Only with JAS	5.51 ± 0.67	−	NA

[a] +, behavior occurred; −, behavior did not occur.
[b] For rate determination, three experiments containing five examples of each type of motility from at least two coverslips per experiment were analyzed. Rates are given as micrometers per second, except for twirling, for which revolutions per second are shown.
[c] Rates for tachyzoite gliding are taken from reference 36.
[d] *, significantly faster ($P < 0.05$) than *T. gondii* tachyzoites by Student's two-tailed *t* test.
[e] NA, not applicable.

and Table 1; see also video 2). Notably, *C. parvum* sporozoites moved more rapidly than did *T. gondii* tachyzoites. The average gliding velocity for *C. parvum* was 5.1 μm/s, approximately three times the average for *T. gondii* tachyzoites (Table 1). Because helical gliding by *C. parvum* occurred rapidly (video 2), it was difficult to specify its precise phases in real time. However, frame-by-frame analysis of helical gliding by *C. parvum* (as shown in Fig. 1D) indicated that the steps involved were similar to those previously described for *T. gondii* (19).

In order to determine whether real-time gliding motility by *C. parvum* depended on actin and myosin, we next studied the effects of cytoskeletal inhibitors on gliding by *C. parvum* sporozoites. Motility by *C. parvum* sporozoites was completely blocked by actin-depolymerizing agents (CD and LatB) and by the myosin inhibitor BDM (data not shown). Treatment with the actin-polymerizing drug JAS completely prevented movement by *C. parvum* sporozoites, despite previous observations that it increases nonproductive motility by *T. gondii* tachyzoites (36).

In conclusion, although gliding motility by *C. parvum* and *T. gondii* clearly depended on stereotypical behaviors driven by an actin-myosin-based motor, there were differences between the two species in the rate of gliding and the responses to jasplakinolide.

Gliding motility by *T. gondii* sporozoites is similar to that of tachyzoites. We were interested in determining if the differences in motility seen between *C. parvum* sporozoites and *T. gondii* tachyzoites were due to species differences or the stage of the parasite. Therefore, for comparison, we analyzed motility by *T. gondii* sporozoites in real time using video microscopy. We found that sporozoite motility was strikingly similar to tachyzoite gliding by *T. gondii*. Identical stereotypical movements were used by tachyzoites and sporozoites: circular gliding (Fig. 2A; video 3), helical gliding (video 4), and clockwise twirling (Fig. 2B; video 5) (all videos are available at http://www.sibleylab.wustl.edu/cptgmovies/). Tachyzoites and sporozoites also moved at approximately the same velocity (Table 2). These movements depended on F-actin and myosin, as evidenced by the fact that the motility of *T. gondii* sporozoites was completely blocked by CD, LatB, and BDM (data not shown). In addition,

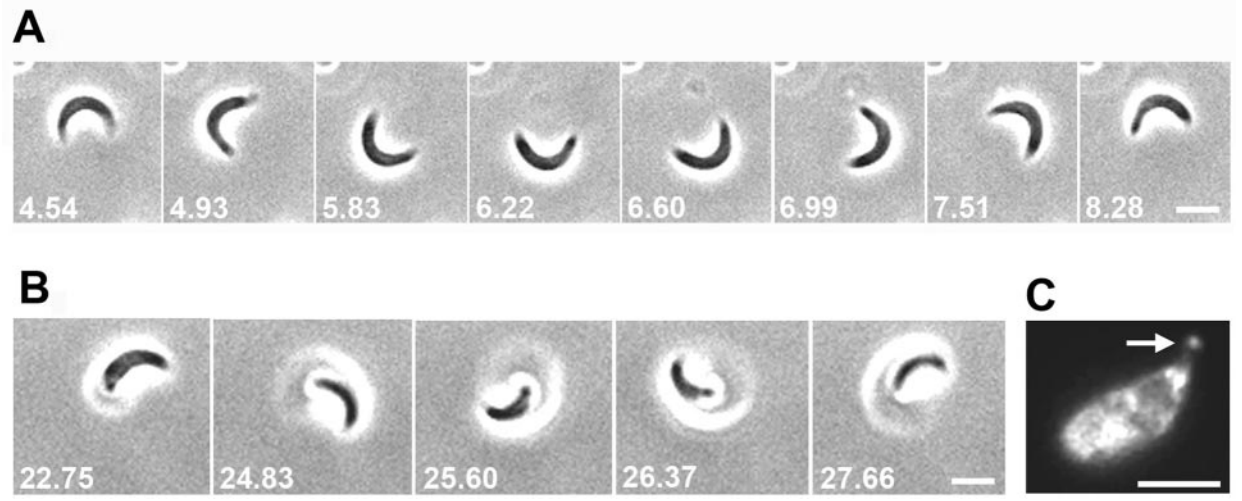

FIG. 2. Gliding motility by *T. gondii* sporozoites. (A and B) Time lapse phase-contrast video microscopy allowed visualization of gliding motility by *T. gondii* sporozoites in real time. Shown are series of frames from movies of circular gliding (video 3) (A) and twirling (video 5) (B) by *T. gondii* sporozoites. Time elapsed is shown in seconds in the lower left corner of each frame. Bars, 5 μm. (C) Upon treatment with 2 μM JAS, *T. gondii* sporozoites formed apical projections of actin (arrow). Actin was visualized using a monoclonal antibody to actin (C4) and a secondary anti-mouse antibody conjugated to Texas Red. Bar, 5 μm.

TABLE 2. Rates of gliding motility by *T. gondii* sporozoites

Behavior	Rate[a] (mean ± SE) of:		
	Sporozoites		Tachyzoites,[c] with 2 μM JAS
	Under control conditions	With 2 μM JAS[b]	
Twirling			
Clockwise	0.25 ± 0.04	0.37 ± 0.03*	0.98 ± 0.36
Counterclockwise	NA	ND[d]	0.88 ± 0.37
Circular gliding	1.37 ± 0.41	ND[e]	NA
Helical gliding	1.65 ± 0.20	NA	NA
Rolling	NA	3.50 ± 0.52*	5.51 ± 0.67

[a] For rate determination, three experiments containing five examples of each type of motility from at least two coverslips per experiment were analyzed. Rates are given as micrometers per second, except for twirling, for which revolutions per second are shown. NA, not applicable; ND, not determined.

[b] *, significantly faster ($P < 0.05$) than under control conditions by Student's two-tailed *t* test.

[c] Rates for tachyzoite gliding are taken from reference 36.

[d] Similar to rate for clockwise twirling.

[e] Rarely occurring.

studies using high concentrations (2 μM) of JAS caused actin to accumulate at the apical ends of ~30% of treated sporozoites (Fig. 2C) and increased the rates of motility of both *T. gondii* tachyzoites and sporozoites (Tables 1 and 2). JAS-treated sporozoites were slightly more capable of carrying out stereotypical movements of gliding than were tachyzoites treated with similar drug concentrations. For example, sporozoites occasionally underwent one step in a cycle of helical gliding before changing direction or type of movement, while tachyzoites could only move back and forth ("roll") in response to JAS. Importantly, however, both sporozoites and tachyzoites moved faster and were able to reverse direction after JAS treatment (Table 2).

Time lapse video analysis of *Cryptosporidium* invasion. To determine if motility by *Cryptosporidium* sporozoites was also involved in cellular invasion, we analyzed the interaction of freshly excysted sporozoites with epithelial cells in vitro. Two types of polarized epithelial cells were used in this analysis: KB100 cells, a human epithelial cell line, and MDCK cells, canine kidney epithelial cells. Time lapse video microscopy indicated that invasion by *Cryptosporidium* sporozoites was rapid, often occurring in ~30 s following initial contact with the host cell (Fig. 3A; video 6). However, in most cases, the parasite did not appear to enter the host cytosol but instead extended beyond the edge of the host cell (Fig. 3B; video 7). Individual sporozoites at times initially penetrated into the cytosol but then reversed direction and returned to the surface of the cell (Fig. 3C; video 8) (all videos are available at http://www.sibleylab.wustl.edu/cptgmovies/). Following invasion, a majority of parasites remained firmly attached but appeared to protrude from the cell surface. As previously observed for *T. gondii* (19, 36), invasion was always preceded by helical gliding while circular gliding did not lead to productive invasion (data not shown).

Rapid invasion leads to membrane engulfment at the cell surface. To determine whether attached and protruding parasites were actually within the host cell membrane, we used a latency assay to monitor their accessibility to antibodies to a cell surface antigen on the sporozoite. Following a short 5-min pulse for invasion, cells were lightly fixed and stained first with a MAb to the sporozoite surface antigen p25 and then with a red dye-conjugated secondary antibody. This step will stain extracellular parasites red, while internalized parasites will be protected from labeling. The monolayer was then permeabilized and restained with a MAb to the sporozoite surface antigen p25 followed by green dye-conjugated secondary antibodies that will label all parasites. The ratio of double-stained (red and green) (external) parasites to green only (internal) parasites provides a sensitive index for invasion. Analysis of *Cryptosporidium* sporozoites invading KB100 cells confirmed that approximately half of the parasites that were cell associated were internalized during this short invasion pulse (Fig. 4A). This rate of entry is roughly equal to that observed in invasion assays employing *T. gondii* (our unpublished observations). Internal parasites, as defined by their selective green staining, were often found to protrude from the edge of the cell (Fig. 4B), indicating that they were enclosed within the host membrane despite the appearance of being peripherally attached. At the points of parasite entry, there were no obvious changes in host cell actin as detected by phalloidin labeling (Fig. 4B).

Invasion by *Cryptosporidium* relies on the parasite's actin cytoskeleton. Previous studies have shown that the invasion of host cells by *T. gondii* is blocked by CD, which also blocks parasite entry into host cells that are fully resistant to the effects of the drug (9). These findings established that invasion requires actin polymerization in the parasite. To test whether *Cryptosporidium* exhibited a similar requirement, we examined the rapid invasion of KB100 (wild-type) and CYT1 (CD-resistant) host cells by using the latency assay described above. The majority of *Cryptosporidium* sporozoites that were associated with KB100 and CYT1 cell monolayers were internalized after 5 min (Fig. 4A and B). However, their ability to enter both wild-type and CD-resistant host cells was almost completely blocked by CD (Fig. 4A and B). Inhibition of entry was evident in the two-color assay by the presence of parasites that remained attached to the cell but were exposed to externally added antibodies (red staining) (Fig. 4B). These results indicate that *Cryptosporidium* requires actin polymerization in the parasite to enter the protective environment of the host cell membrane.

DISCUSSION

Here we demonstrate that *C. parvum* sporozoites display gliding behaviors similar to those previously described for other apicomplexans. The motility of *Cryptosporidium* sporozoites was faster than that of either tachyzoites or sporozoites of *T. gondii*. *Cryptosporidium* motility was blocked by BDM, LatB, or CD, indicating requirements for both myosin activity and polymerized actin. Time lapse video microscopy revealed that gliding motility led to invasion of host cells but that this process differed significantly from invasion by *T. gondii*. While *T. gondii* tachyzoites invade a vacuole within the cytosol, *Cryptosporidium* sporozoites invaded at the cell periphery but were nonetheless enclosed within the host cell membrane. Host cell invasion required actin polymerization by the parasite but evidently not the host, indicating that a common mechanism drives invasion by diverse apicomplexan parasites.

Our studies using *C. parvum* are the first real-time characterizations of its motility. Gliding motility occurred in both

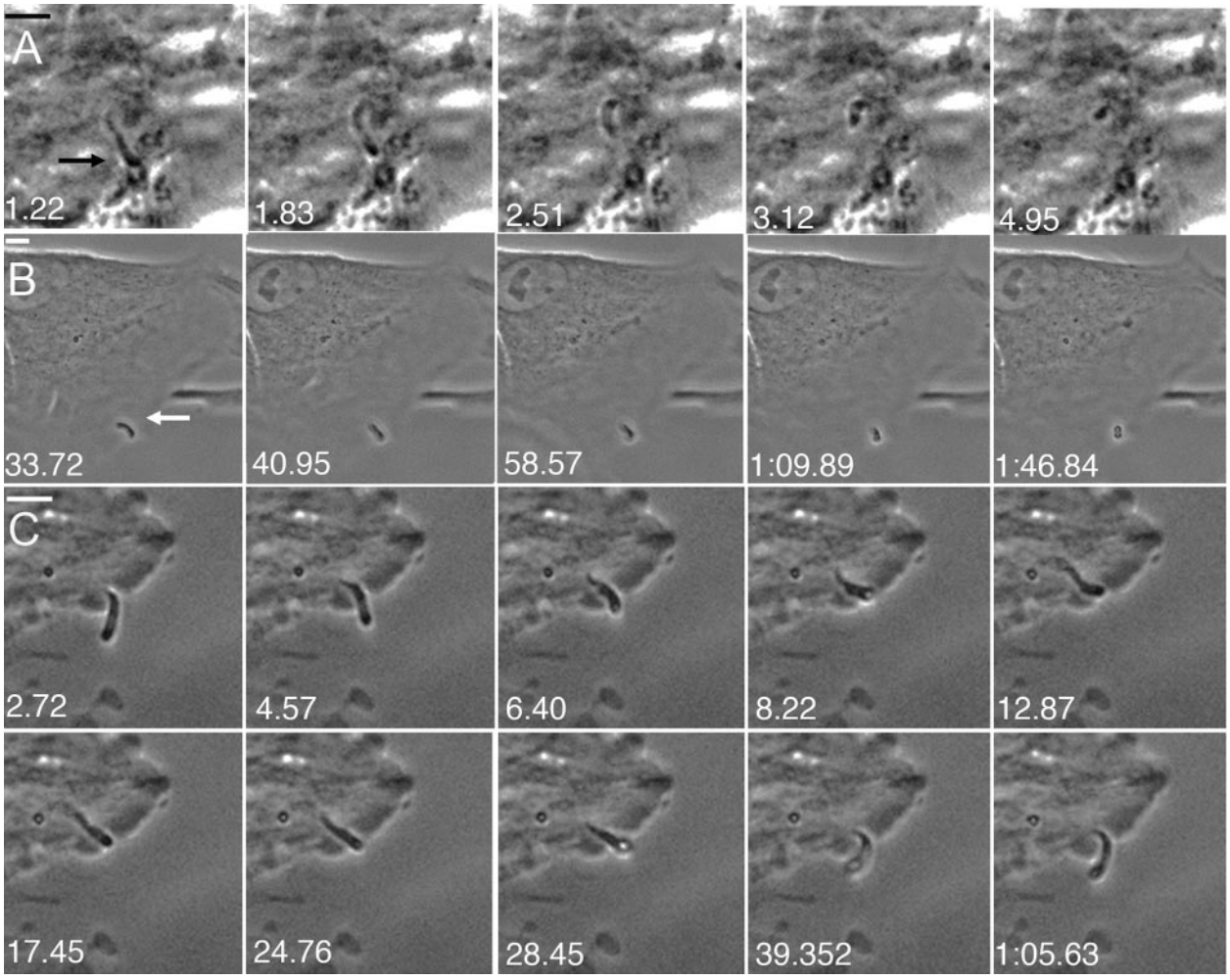

FIG. 3. Real-time invasion of host cells by *C. parvum*. (A) *C. parvum* invading a KB100 epithelial cell (video 6). The parasite was gliding on top of the cell monolayer prior to invasion. (B) *C. parvum* invading an MDCK cell (video 7). The parasite approached the edge of the cell and then invaded just under the cell membrane. (C) *C. parvum* appearing to enter and exit a KB100 cell (video 8). Bar, 5 μm. All images are from video 3. Arrows indicate the position of the parasite in the first frame.

circular patterns, as described previously from static assays (2), and helical patterns, previously described for *T. gondii*. Helical, but not circular, gliding precedes cell entry by *T. gondii* (19, 28) and *Plasmodium* (35), and a similar relationship was also observed here for *Cryptosporidium*. During gliding, *C. parvum* exhibited movements similar to those exhibited by *T. gondii*, except that it was not observed to twirl on its posterior end. Perhaps this difference is due to the relative shape of the two organisms; *C. parvum* is about half the diameter of *T. gondii*. Consequently, it may lack the ability to generate the force necessary to pivot about the posterior end, or, alternatively, it may lack the rigidity necessary for standing upright. The importance of twirling in 3-dimensional settings has not been examined, and therefore it is uncertain if it plays any role in vivo.

Motility by *C. parvum* occurred almost three times faster than *T. gondii* motility under similar situations. Interestingly, this matches the enhanced speed with which *T. gondii* tachyzoites move after treatment with jasplakinolide (Table 2) (36). It also corresponds to the rate of purified TgMyoA sliding along actin filaments (20). Since TgMyoA is a nonprocessive motor without a clear method of activation (27), we have previously suggested that the rate-limiting step for gliding motility by apicomplexans is actin polymerization (36). The faster motility by *Cryptosporidium* sporozoites may indicate that they naturally have a higher proportion of polymerized actin, which is also consistent with their being less responsive to the effects of JAS.

C. parvum and *Plasmodium* sp. sporozoites move more rapidly than *T. gondii* tachyzoites (18), suggesting that this may be a general trait of sporozoites. However, when analyzed by time lapse video microscopy, *T. gondii* sporozoites moved at speeds comparable to those of tachyzoites, indicating that these differences are species specific, not stage specific. *T. gondii* sporozoites displayed the same stereotypical movements as tachyzoites despite minor variations in susceptibility to inhibitors. For example, *T. gondii* sporozoites were slightly less susceptible to JAS and were still able to carry out one cycle of helical gliding after treatment, while tachyzoites were unable to proceed forward (30).

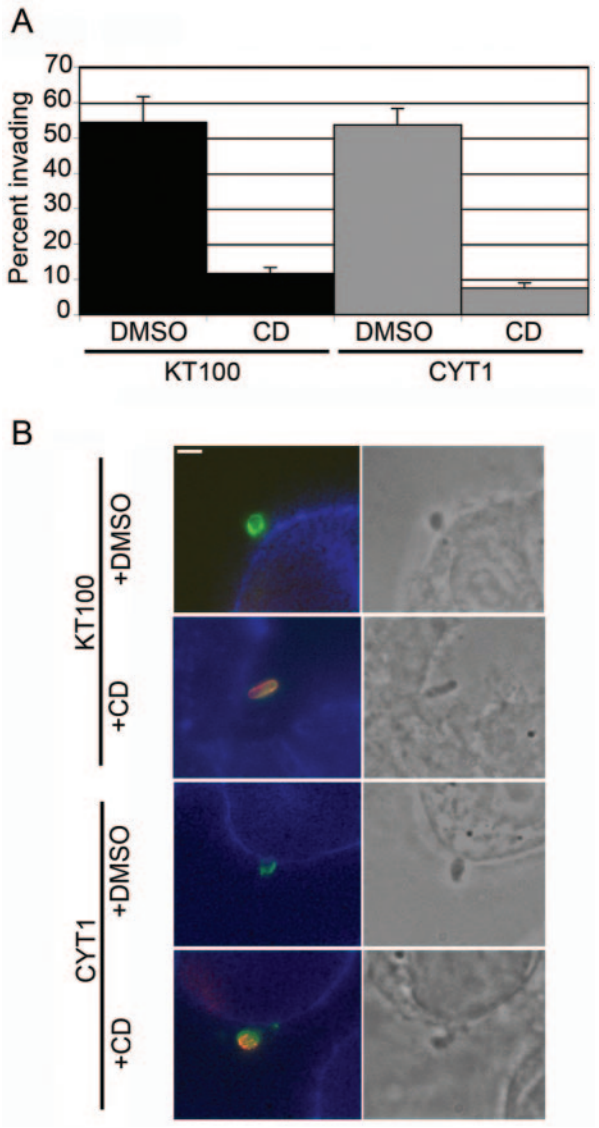

FIG. 4. *C. parvum* invasion depends on parasite actin but not on host cell actin. (A) *C. parvum* efficiently invaded KB and CYT1 cells in the absence of drug (DMSO control). In the presence of CD, the percentage of parasites invading KB100 cells was reduced from 54 to 11% ($P < 0.05$), and the percentage of parasites invading CYT1 cells, which are resistant to CD, was reduced from 53 to 7% ($P < 0.05$). The percentage invading was calculated using a two-color latency assay described in the legend to panel B. Results shown are means ± SE ($n = 3$). (B) A two-color immunofluorescence assay demonstrated that *C. parvum* was able to efficiently invade host cells yet remained at the cell surface and often protruded away from the cell surface despite being enveloped within the host cell membrane (DMSO control). *Cryptosporidium* was not able to invade either control or CD-resistant host cells in the presence of CD. Parasites were allowed to enter KB100 or CYT1 cells, fixed, and stained by using the antibody to surface p25 followed by secondary antibodies conjugated to Alexa 594 (red). Cells were then permeabilized and stained with anti-p25 followed by secondary antibodies conjugated to Alexa 488 (green). External parasites were labeled red and green (and appear orange-yellow in most cases), and parasites that had invaded cells were labeled green. Host cell actin was labeled with phalloidin conjugated to Alexa 350 (blue). Shown are merged 3-color immunofluorescence images (left) and the corresponding phase images (right). Bar, 5 μm.

Previous studies have established that sporozoites of *T. gondii* have a much greater capacity to migrate rapidly through host tissues than bradyzoites (10, 13). We have not examined the motility of bradyzoites in vitro but would expect their behaviors to be similar to those of tachyzoites, since they are able to invade similar types of cells in vitro. The enhanced dissemination ability of sporozoites suggests that additional factors must contribute to their rapid spread in vivo. Following infection in the gut, parasites must traverse the epithelial monolayer, cross the basement membrane, and migrate through the lamina propria in order to reach the circulatory system (4). While in vivo studies have shown that *T. gondii* can migrate deep into the intestinal submucosal tissue (5, 10, 13), it is unclear if parasites disseminate while extracellular or by gaining access into migrating leukocytes that then traffic to distant sites. In vitro studies have established that virulent strains of *T. gondii* have an enhanced capacity to migrate directly across biological barriers in vitro (3); however, this mechanism and an intracellular dispersal route are not mutually exclusive.

Although previous studies have suggested that F-actin is necessary for trail formation by *C. parvum* (17), these experiments relied solely on static assays. We have extended these observations to examine the behavior of *Cryptosporidium* sporozoites during both gliding and host cell invasion by using time lapse video microscopy. These observations reveal that *Cryptosporidium* utilizes a conserved process of gliding motility that also results in a unique mode of cell entry. Instead of penetrating into a vacuole within the host cell cytosol, the parasite becomes enveloped within a membrane-bound compartment while remaining at the cell periphery. A majority of parasites interacting with host cells during a short invasion pulse of 5 min were able to complete the entry process, as shown by their protection from antibody labeling. This mode of entry coincides with the development of *Cryptosporidium*, which proceeds within an apical protrusion from the host cell surface. Our studies using inhibitors and CD-resistant host cells reveal that the successful engulfment of the parasite requires actin polymerization on the part of the parasite, but evidently not by the host cell. Collectively, these findings indicate that host cell internalization is driven by the parasite actin cytoskeleton.

Our studies might appear to contradict earlier findings that indicate that *C. parvum* induces changes in host cell actin after infection (9, 10). However, our experiments have been conducted at a time point very different from those reported previously. We specifically examined the early events (5 min) in entry, while previous studies examined infection only after 24 h. We observed no change in host cell actin during invasion of host cells by the parasite. Furthermore, host cell actin is not alone sufficient to drive engulfment, as evidenced by the fact that *Cryptosporidium* fails to enter CD-resistant host cells in the presence of drug. Our findings strongly indicate that initial entry into the host cell is driven by actin-dependent gliding motility, much the same as it is for *T. gondii* and *Plasmodium* spp. (32). However, it is also clear that major alterations occur in the underlying host cell cytoskeleton following infection. The formation of an actin-rich pedestal is important for the growth and development of *Cryptosporidium*, as shown by studies that disrupt host actin dynamics (15). Further studies will be

TABLE 3. Homologues of actin-myosin cytoskeleton genes in *T. gondii* and *C. parvum*[a]

Gene product	Gene	Homologue in:		% Identity	*P*
		T. gondii	*C. parvum*		
Actin	*ACT1*	P53476	AAM28417	88	0.0
Myosin A	*MYOA*	O00934	EAK90372	56	0.0
Myosin light chain kinase	*MLC1*	AAL08211	EAK90019	28	$1e^{-15}$
Capping protein β	*CapZb*	AY71398	EAK88546	24	$7e^{-06}$
Actin-depolymerizing factor	*ADF*	AAC47717	EAK88221	32	$7e^{-15}$
Profilin	*PRF*	AY937257	EAL35531[b]	45	$1e^{-12}$

[a] Comparison was done by BLASTP using *T. gondii* genes compared against GenBank by using default settings.

[b] Predicted protein found in *Cryptosporidium hominis*, the homologue in *C. parvum* was identified by TBLASTN against http://CryptoDB.org (CpIOWA III s2:345790-466126).

required to define the mechanisms that induce changes in host cell actin and to resolve the precise time frame when such changes are initiated.

The phylum Apicomplexa is highly diverse and contains some 5,000 species, only a few of which are studied. *Cryptosporidium* represents a fairly early branching member of this group, more closely related to gregarines than to *Plasmodium* or *Toxoplasma* (6). The conservation of an actin-based system for motility and cell invasion in *Cryptosporidium* indicates that this process is likely common to most members of the phylum. *C. parvum* possesses homologues to *T. gondii* actin and myosin that are 85% (22) and 57% identical, respectively (Table 3). Furthermore, TBLASTN searches of the CryptoDB (http://CryptoDB.org/) and NCBI databases identified clear homologues of myosin light chain kinase, a component of the myosin motor complex in *T. gondii* (21), and several actin polymerization regulatory proteins from *T. gondii*, including actin-depolymerizing factor (ADF) (1), profilin, and capping protein (CapZβ) (Table 3). While these components have not been fully characterized in parasites, our results suggest that a common process of gliding motility is based on a relatively simple set of conserved cytoskeletal proteins in the Apicomplexa.

Gliding motility is an actin- and myosin-dependent process that is conserved throughout the life cycle and different species of the Apicomplexa. The actin dynamics in these parasites are also highly unusual, with a majority of actin being retained in a monomeric form (8). Due to their unique reliance on polymerization of new filaments for gliding (36), these organisms are acutely sensitive to the inhibitors of actin polymerization. Because no treatments to clear infection by apicomplexans such as *C. parvum* exist (7), a better understanding of the mechanism behind the gliding motility of these medically important parasites may one day be exploited to develop pharmaceutical agents.

ACKNOWLEDGMENTS

We thank Michael White (Montana State University) for the excystation protocol for *T. gondii* oocysts and Julie Suetterlin for expert technical assistance.

This work was supported by NIH Institutional Training Grant AI017172-19 and NRSA Medical Scientist Training Grant 5T32GM07200-30 (to D.M.W.), NIH grant AI34036 (to L.D.S), and the Burroughs Wellcome Fund (to L.D.S).

REFERENCES

1. **Allen, M. L., J. M. Dobrowolski, H. Muller, L. D. Sibley, and T. E. Mansour.** 1997. Cloning and characterization of actin depolymerizing factor from *Toxoplasma gondii*. Mol. Biochem. Parasitol. **88:**43–52.
2. **Arrowood, M. J., C. R. Sterling, and M. C. Healey.** 1991. Immunofluorescent microscopical visualization of trails left by gliding *Cryptosporidium parvum* sporozoites. J. Parasitol. **77:**315–317.
3. **Barragan, A., F. Brossier, and L. D. Sibley.** 2005. Transepithelial migration of *Toxoplasma gondii* involves an interaction of intercellular adhesion molecule 1 (ICAM-1) with the parasite adhesin MIC2. Cell. Microbiol. **7:**561–568.
4. **Barragan, A., and L. D. Sibley.** 2003. Migration of *Toxoplasma gondii* across biological barriers. Trends Microbiol. **11:**426–430.
5. **Barragan, A., and L. D. Sibley.** 2002. Transepithelial migration of *Toxoplasma gondii* is linked to parasite motility and virulence. J. Exp. Med. **195:**1625–1633.
6. **Carreno, R. A., D. S. Martin, and J. R. Barta.** 1999. *Cryptosporidium* is more closely related to the gregarines than to coccidia as shown by phylogenetic analysis of apicomplexan parasites inferred using small-subunit ribosomal RNA gene sequences. Parasitol. Res. **85:**899–904.
7. **Clark, D. P., and C. L. Sears.** 1996. The pathogenesis of cryptosporidiosis. Parasitol. Today **12:**221–225.
8. **Dobrowolski, J. M., I. R. Niesman, and L. D. Sibley.** 1997. Actin in the parasite *Toxoplasma gondii* is encoded by a single copy gene, *ACT1* and exists primarily in a globular form. Cell Motil. Cytoskeleton **37:**253–262.
9. **Dobrowolski, J. M., and L. D. Sibley.** 1996. Toxoplasma invasion of mammalian cells is powered by the actin cytoskeleton of the parasite. Cell **84:**933–939.
10. **Dubey, J. P.** 1997. Bradyzoite-induced murine toxoplasmosis: stage conversion pathogenesis, and tissue cyst formation in mice fed bradyzoites of different strains of *Toxoplasma gondii*. J. Eukaryot. Microbiol. **44:**592–602.
11. **Dubey, J. P.** 1977. *Toxoplasma*, *Hammondia*, *Besniotia*, *Sarcocystis*, and other tissue cyst-forming coccidia of man and animals, p. 101–237. *In* J. P. Kreier (ed.), Parasitic protozoa. Academic Press, New York, N.Y.
12. **Dubey, J. P., N. L. Miller, and J. K. Frenkel.** 1970. The *Toxoplasma gondii* oocyst from cat feces. J. Exp. Med. **132:**636–662.
13. **Dubey, J. P., C. A. Speer, S. K. Shen, O. C. H. Kwok, and J. A. Blixt.** 1997. Oocyst-induced murine toxoplasmosis: life cycle, pathogenicity, and stage conversion in mice fed *Toxoplasma gondii* oocysts. J. Parasitol. **83:**870–882.
14. **Elliott, D. A., and D. P. Clark.** 2000. *Cryptosporidium parvum* induces host cell actin accumulation at the host-parasite interface. Infect. Immun. **68:**2315–2322.
15. **Elliott, D. A., D. J. Coleman, M. A. Lane, R. C. May, L. M. Machesky, and D. P. Clark.** 2001. *Cryptosporidium parvum* infection requires host cell actin polymerization. Infect. Immun. **69:**5940–5942.
16. **Entzeroth, R., G. Zgrzebski, and J. F. Dubremetz.** 1989. Secretion of trails during gliding motility of *Eimeria nieschulzi* (Apicomplexa, Coccidia) sporozoites visualized by a monoclonal antibody and immuno-gold-silver enhancement. Parasitol. Res. **76:**174–175.
17. **Forney, J. R., D. K. Vaughan, S. Yang, and M. C. Healey.** 1998. Actin-dependent motility in *Cryptosporidium parvum* sporozoites. J. Parasitol. **84:**908–913.
18. **Frischknecht, F., P. Baldacci, B. Martin, C. Zimmer, S. Thiberge, J. C. Olivo-Marin, S. L. Shorte, and R. Ménard.** 2004. Imaging movement of malaria parasites during transmission by anopheles mosquitoes. Cell. Microbiol. **6:**687–694.
19. **Håkansson, S., H. Morisaki, J. E. Heuser, and L. D. Sibley.** 1999. Time-lapse video microscopy of gliding motility in *Toxoplasma gondii* reveals a novel, biphasic mechanism of cell locomotion. Mol. Biol. Cell **10:**3539–3547.
20. **Herm-Gotz, A., S. Weiss, R. Stratmann, S. Fujita-Becker, C. Ruff, E. Meyhofer, T. Soldati, D. J. Manstein, M. A. Geeves, and D. Soldati.** 2002. *Toxoplasma gondii* myosin A and its light chain: a fast, single-headed, plus-end-directed motor. EMBO J. **21:**2149–2158.
21. **Keeley, A., and D. Soldati.** 2004. The glideosome: a molecular machine powering motility and host-cell invasion by Apicomplexa. Trends Cell Biol. **14:**528–532.
22. **Kim, K., L. Gooze, C. Petersen, J. Gut, and R. G. Nelson.** 1992. Isolation, sequence and molecular karyotype analysis of the actin gene of *Cryptosporidum parvum*. Mol. Biochem. Parasitol. **50:**105–114.
23. **Kim, K., and L. M. Weiss.** 2004. *Toxoplasma gondii*: the model apicomplexan. Int. J. Parasitol. **34:**423–432.
24. **King, C. A.** 1988. Cell motility of sporozoan protozoa. Parasitol. Today **11:**315–318.
25. **King, C. A.** 1981. Cell surface interaction of the protozoan Gregarina with concanavalin A beads: implications for models of gregarine gliding. Cell Biol. Int. Rep. **5:**297–305.
26. **Liu, C., V. Vigdorovich, V. Kapur, and M. S. Abrahamsen.** 1999. A random survey of the *Cryptosporidium parvum* genome. Infect. Immun. **67:**3960–3969.
27. **Meissner, M., D. Schluter, and D. Soldati.** 2002. Role of *Toxoplasma gondii* myosin A in powering parasite gliding and host cell invasion. Science **298:**837–840.

28. **Morisaki, J. H., J. E. Heuser, and L. D. Sibley.** 1995. Invasion of *Toxoplasma gondii* occurs by active penetration of the host cell. J. Cell Sci. **108:**2457–2464.
29. **Morrissette, N. S., and L. D. Sibley.** 2002. Cytoskeleton of apicomplexan parasites. Microbiol. Mol. Biol. Rev. **66:**21–38.
30. **Petersen, C. A.** 1993. Cellular biology of *Cryptosporidium parvum*. Parasitol. Today **9:**87–91.
31. **Shaw, M. K., and L. G. Tilney.** 1999. Induction of an acrosomal process in *Toxoplasma gondii*: visualization of actin filaments in a protozoan parasite. Proc. Natl. Acad. Sci. USA **96:**9095–9099.
32. **Sibley, L. D.** 2004. Invasion strategies of intracellular parasites. Science **304:**248–253.
33. **Thulin, J. D., M. Kuhlenschmidt, M. D. Rolsma, W. L. Current, and H. B. Gelberg.** 1994. An intestinal zenograph model for *Cryptosporidium parvum* infection. Infect. Immun. **62:**329–331.
34. **Toyama, S., and S. Toyama.** 1988. Functional alterations in β′-actin from a KB cell mutant resistant to cytochalasin B. J. Cell Biol. **107:**1499–1504.
35. **Vanderberg, J. P., S. Chew, and M. J. Stewart.** 1990. *Plasmodium* sporozoite interactions with macrophages *in vitro*: a videomicroscopic analysis. J. Protozool. **37:**528–536.
36. **Wetzel, D. M., S. Håkansson, K. Hu, D. S. Roos, and L. D. Sibley.** 2003. Actin filament polymerization regulates gliding motility by apicomplexan parasites. Mol. Biol. Cell **14:**396–406.

Editor: W. A. Petri, Jr.